



# MATERIALS CHEMISTRY

---

## FRONTIERS



CHINESE  
CHEMICAL  
SOCIETY



ROYAL SOCIETY  
OF CHEMISTRY

[rsc.li/frontiers-materials](https://rsc.li/frontiers-materials)

## REVIEW

View Article Online  
View Journal | View IssueCite this: *Mater. Chem. Front.*,  
2020, 4, 2499

# Chiral conducting polymer nanomaterials: synthesis and applications in enantioselective recognition

Chuanqiang Zhou, <sup>a</sup> Xiaohuan Sun <sup>b</sup> and Jie Han \*<sup>b</sup>

Chiral conducting polymer (CCP) nanomaterials have been the subject of several studies due to their unique electrical and chiroptical properties as well as promising applications. This review mainly summarizes the advances made in the synthesis and applications of CCP nanomaterials in the past two decades. According to the origin of chirality, the fabrication of CCP nanomaterials can be distinguished into chiral induction and achiral preparation strategies. Under the induction of chiral factors (such as chiral substituent, chiral doping acid, or chiral template), the chirality of the conducting polymer (CP) nanomaterials is induced by the chirality transfer from the chiral factors to the CP nanomaterials. In achiral preparation systems, the asymmetrical assembly of CPs results in the supramolecular chirality of the CP nanomaterials. Subsequently, the applications of CCP nanomaterials in enantioselective recognition are reviewed. Besides, the challenges and prospects for constructing advanced CCP nanomaterials are discussed.

Received 29th February 2020,  
Accepted 19th May 2020

DOI: 10.1039/d0qm00103a

rsc.li/frontiers-materials

## 1. Introduction

Conducting polymers (CPs) possess a long  $\pi$ -conjugated electron system in their molecular chain structures, and they exhibit unique electrical properties that cover the entire insulator–semiconductor–metal range. In general, the redox features of CPs can be facilely

adjusted *via* reversible acid/base doping/dedoping processes. For example, polyaniline (PANI) may reversibly change its oxidation state by doping/dedoping or oxidation/reduction routes.<sup>1</sup> Also, the organic nature of CPs can be conveniently tuned by appending functional groups to the polymer backbone. The reversible redox feature and tunable organic nature of CPs offer efficient approaches to control their electrical and optical properties.<sup>2</sup> Moreover, many approaches have been reported for the fabrication of CP nanomaterials with various morphologies such as nanofibers, nanotubes, and nanofilms, which can enhance their properties.<sup>3,4</sup>

<sup>a</sup> Testing Center, Yangzhou University, Yangzhou, 225002 Jiangsu, P. R. China<sup>b</sup> School of Chemistry and Chemical Engineering, Yangzhou University, Yangzhou, 225002 Jiangsu, P. R. China. E-mail: hanjie@yzu.edu.cn**Chuanqiang Zhou**

His main research activities focus on the controllable fabrication and application of conducting polymer nanomaterials.

Chuanqiang Zhou received his BS (2004) and PhD (2009) degrees from the School of Chemistry and Chemical Engineering, Yangzhou University, China. He joined the Centre national de la recherche scientifique (CNRS), Centre de Recherche sur la Matière Divisée, Orléans, France, as a postdoctoral researcher in 2018–2010. Since 2011, he worked at the Testing Center, Yangzhou University, China. Since 2017, he has been an Associate Researcher.

**Xiaohuan Sun**

Xiaohuan Sun received her BS degree in 2015 from the School of Chemistry and Chemical Engineering, Shannxi Normal University, and her PhD degree in 2019 from the Department of Chemical Science, University of Padova, Italy. Afterward, she got a lectureship in the School of Chemistry and Chemical Engineering, Yangzhou University. Her main research interests focus on photophysical chemistry, gold-nanoparticle-based NMR sensing, and enantioselective separation.

**Table 1** Comparison of different strategies involved in the synthesis of CCP nanomaterials

Method	Feature	Advantage	Limitation
Chiral preparation	Induction of chiral substituent	Monomer bearing chiral substituent leading to intrinsic chirality of CPs after polymerization	Stable chirality under various environment conditions
	Induction of chiral doping acid	Introducing chirality in CPs <i>via</i> intermolecular interactions with chiral doping acid	Easy to operate utilizing doping characters of CPs, or intermolecular interactions
Achiral preparation	Induction of chiral template	Chirality transfer from chiral template to CPs after template-assisted polymerization	Controlling chirality of CP nanomaterials by chiral template
		Generation of chirality for CPs in specially appointed achiral system through asymmetrical assembly	Economic and environmentally friendly process

Therefore, CP materials have exhibited diverse applications in different fields, and they have been suggested to be one of the most promising functional materials.<sup>5,6</sup>

Chirality—which is ubiquitous in nature—often contributes toward the exceptional specificity of metabolic processes in the biosome.<sup>7</sup> When artificial materials possess a chiral feature, chiral optical activities can become an additional functionality in the materials.<sup>8,9</sup> Endowing CP materials with chirality can result in multifunctionality and may generate new interdisciplinary areas such as chiral electronics, chiral optics, and chiral optoelectronics. Chiral conducting polymers (CCPs) exhibit not only high electrical conductivity, but also exceptional chiroptical properties that open new potential applications in chiral electronic devices, electrochemical asymmetric catalysis, electrochemical chiral sensing, or enantioselective separation of enantiomeric drugs.<sup>10,11</sup> Among these applications of CCP nanomaterials, enantioselective recognition is very important for obtaining pure enantiomers in their mixtures. Since enantiomers have identical physicochemical properties and therefore also share the same electrochemical reactivity, they can only be discriminated by the electron transfer process occurring in an enantiopure chiral environment.

Due to their potential applications, CCP nanomaterials have garnered increasing attention in the past two decades. Some reviews dealing with the preparation, properties, and applications of CCPs have been reported in recent years. For example, Kane-Maguire *et al.* summarized the preparation and properties of CCPs.<sup>10</sup> Yang *et al.* summarized the chirality transfer from molecules to the supramolecular structures of CPs.<sup>11</sup> Multi-component chirality in conjugated polymers and their properties have been reviewed by Verswyvel *et al.*<sup>12</sup> The applications of CCPs in the fields of electrochemical enantioselective recognition<sup>13</sup> and spin filter<sup>14</sup> have also been recently reviewed. Although many studies about CCPs have been reported to date, to purposively design and synthesize chiral nanostructures of CPs is still a scientific challenge. For better understanding the recent developments and arousing new research ideas in this field, it is highly desirable to systematically summarize the syntheses and applications of CCP nanomaterials.

In this review, we mainly focus on new developments in the preparation of CCP nanomaterials and their applications in enantioselective separation and sensing developed in the past two decades. This review aims to provide a general overview of the recent advances in this field and stimulate new research ideas for the designing and synthesis of CCP nanomaterials with worthwhile properties and promising applications. Overall, the fabrication of CCP nanomaterials can be distinguished into chiral and achiral preparation strategies, as listed in Table 1. The chiral preparation of CCP includes chiral substituent-induced, chiral doping-acid-induced, and chiral template-induced methods. Generally, bearing chiral substituents into monomer units is a crucial factor for the chiral substituent-induced fabrication, while chiral doping-acid- or chiral template-induced methods require compact interactions between the monomers and chiral acids or templates. Achiral preparation of CCPs is significant due to the generation of chirality and economic processability, but the type of chiral control is still a challenge.

**Jie Han**

*Jie Han received his BS (2003) and PhD (2008) degrees from the School of Chemistry and Chemical Engineering, Yangzhou University, China. Then, he began his academic career at the School of Chemistry and Chemical Engineering, Yangzhou University, China. He joined the University of California, Riverside, United States, as a Visiting Scholar in 2012. Since 2015, he has been a Full Professor at the School of*

*Chemistry and Chemical Engineering, Yangzhou University. His main research activities focus on the controllable synthesis of conducting-polymer-based functional hybrids for catalysis, energy conversion and storage, and biomedical applications.*

## 2. Synthesis of CCP nanomaterials

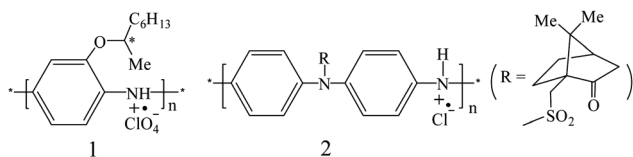
### 2.1. Chiral preparation

#### 2.1.1. Induction of chiral substituents

**2.1.1.1. Chiral PANI bearing a chiral substituent.** In order to induce chirality, chiral substituents can be introduced to the

repeat units of CPs *via* the formation of a covalent bond. For example, Goto<sup>15</sup> were the first to synthesize an aniline monomer bearing a chiral substituent and then prepared emeraldine salts **1** with strong optical activity by the interfacial polymerization with ammonium persulfate (APS) as the oxidant in mixed solvents.

Besides the induction of a chiral substituent into a monomer, the chiral substituent can also be grafted onto PANI polymer chains. Reece *et al.* reported the preparation of chiral *N*-substituted emeraldine salt **2** *via* the reaction of the emeraldine base with (1*S*)-(+)-10-camphorsulfonyl chloride in mixed organic solvents.<sup>16</sup> Two bands were observed at 405 and 460 nm in the circular dichroism (CD) spectrum of the product in *N*-methyl-2-pyrrolidone (NMP) solvent, which was related to the UV-vis absorption at 435 nm. The signals in the CD and UV-vis spectra could confirm the chirality of the obtained PANI caused by a covalently attached group. After dedoping by a basic solution, the chiral emeraldine salts with a chiral character were transferred into emeraldine bases, where the chiral character could be retained. However, the grafting of the chiral substituent to the polymer was seldom reported for other CPs [polypyrrole (PPY) or polythiophene (PTH)].



**2.1.1.2. Chiral PPY bearing a chiral substituent.** In earlier studies, Pleus *et al.* synthesized PPYs **3** and **4** by grafting chiral side chains at the 3-position and ring N atom of the pyrrole units, respectively.<sup>17</sup> Initially, CD measurements were not performed, but the enantioselective properties could be determined by the cyclic voltammetry (CV) data when (+)- or (-)-camphorsulfonic acid (CSA) ions existed in the testing system.



With FeCl<sub>3</sub> as the oxidant, Costello *et al.* synthesized several PPYs bearing chiral ester substituents *via* the chemical polymerization of pyrrole monomers **5** in water/CH<sub>3</sub>CN [R = (*R*)- and (*S*)-menthol, -*boc*-alaninol, and -phenylethanol].<sup>18</sup> The electropolymerization method was also used to prepare chiral PPYs **6** and **7** in an organic solvent when their monomers were grafted with chiral ester units at the ring N atoms.<sup>19</sup> If the chiral CSA ions existed in the preparation system, their chiral discrimination toward chiral ions could be observed by measuring the changes in the *S/N* ratios.

**2.1.1.3. Chiral PTH bearing a chiral substituent.** Using the McCullough methodology, Koeckelberghs *et al.* prepared chiral poly[3-(4-alkoxythiophene)] and studied the two-step aggregation processes of this polymer.<sup>20</sup> They found that the evaporation ratio of the solvent could affect the assembly and deposition of the polymer chains. If the solvent was slowly evaporated, poly[3-(4-alkoxythiophene)] chains could form an ordered and chiral film, while the achiral film comprising random coils would be generated when the solvent was rapidly evaporated. By controlling the evaporation rate of the solvent, an intermediate state between the random coils and aggregates could be observed in the film, which comprised rigid and coplanar polymer strands. Moreover, they reported a chiral and regioregular PTH substituted with a chiral and conjugated group using a coupling reaction method.<sup>21</sup> When the polymer backbone aggregated, these conjugated and chiral side chains would become asymmetrically (chirally) organized.

Further, a modified McCullough method was developed by Koeckelberghs *et al.* to prepare regioregular PTH **8**.<sup>22</sup> The film of PTH **8** showed an obvious Cotton effect in the CD spectrum, corresponding to the  $\pi$ - $\pi^*$  absorption band, where a large chiral anisotropy factor was found ( $g = 10^{-2}$ ) at 745 nm. Chiral PTH **8** in the neutral form could be oxidized by iodine into the oxidized form, while oxidized PTH **8** could also be reduced to the neutral form when treated with hydrazine.



The modified McCullough route was also used to produce chiral PTHs **9** and **10** by grafting chiral methylbutyl and ethylhexyl sides, respectively.<sup>23</sup> It was found that both PTH **9** and **10** exhibited good chiroptical properties. For bulkier **10** in a xylene/DMF solution,  $g$  was as high as  $1.8 \times 10^{-2}$  at 625 nm, corresponding to the  $\pi$ - $\pi^*$  absorption band, which was  $2.9 \times 10^{-2}$  as this polymer formed a thin film in toluene. PTH **9** and **10** could also be oxidized by iodine into doped salts with a chiral character. Besides, Stille-type coupling reactions were also reported to produce chiral PTHs, such as PTH **11** and **12**, which could form a film from an organic solvent and exhibited excellent optical activity.<sup>24</sup> Other chiral PTHs bearing different chiral substituents<sup>25,26</sup> have also been synthesized by different methods. Recently, the influence of the position of a chiral substituent on the conformation of the undecathiophene chain has been studied using the density functional theory method.<sup>27</sup>

**2.1.2. Induction of a chiral doping acid.** CPs are normally synthesized in the presence of a doping acid; therefore, it is reasonable to assume that the chirality of CPs can also be induced by a chiral doping acid. Although there are no chiral carbon atoms in CP chains, the optical activities of PANI can stem from the asymmetric conformation of CP backbone caused by the doping of a chiral acid. In general, the induction of chirality in CP nanomaterials by means of a doping acid can be summarized as follows: (i) induction of chiral doping acid through the electrochemical polymerization route, (ii) induction of chiral doping acid through the chemical polymerization route, and (iii) induction of chiral doping acid through self-assembly.

**2.1.2.1. Induction of chiral doping acid through the electrochemical polymerization route.** Zhang *et al.* reported that enantiomeric CSA could induce optical activity in PANI *via* electrochemical preparation.<sup>28</sup> They prepared optically active PANI films on various substrates (working electrodes) such as Au, indium tin oxide, and graphite by the electrodeposition method in the CSA solution by adjusting the potential. In the two-step potential method with unchanged 2nd potential (0.7 V), the 1st potentials were set to 0.85, 0.95, and 1.05 V

for graphite, Au, and indium tin oxide electrodes, respectively. The setting potentials were marginally higher than that of aniline oxidation for triggering the polymerization reaction of aniline. In the electrodeposition process, the stereochemical selectivity of PANI chains could be achieved when they were deposited on different electron substrates with chiral CSA. The chirality of the PANI film was further proven by the Cotton effects evident in the CD spectra, which showed symmetrical CD curves for *S*-CSA and *R*-CSA. Besides, it was found that once the oxidation polymerization was initiated, the effect of different electrodes on the polymerization of aniline was relatively marginal. The obtained PANI films showed mat-like porous structures, which were knitted by twisted nanofibers.

Besides chiral PANI films, helical PANI nanofibers were also prepared by means of electrochemical polymerization and using enantiomeric CSA as the doping acid. Weng *et al.* synthesized helical PANI nanofibers *via* a direct electrochemical method in the presence of *S*-CSA or *R*-CSA as the dopant.<sup>29</sup> They performed electrochemical polymerization where indium tin oxide, platinum, and saturated calomel electrodes were used as the working, counter, and reference electrodes, respectively. The prepared product was composed of twisted nanofibers with diameters of approximately 100 nm and length of several microns. Using *S*-CSA as the doping acid, the prepared product mainly comprised right-handed nanofibers, while left-handed PANI nanofibers were found to be the main morphology in the product afforded when *R*-CSA was used as the doping acid (Fig. 1). It was demonstrated that the chirality of PANI could be retained when CSA was removed *via* a dedoping process. Moreover, the chiroptical properties of the products could be reversibly adjusted by facily tuning the potentials used in the preparation process.

Steric effects introduced by the substituent on the structure and chiral activity were reported by Lee *et al.*<sup>30</sup> They used the potentiodynamic method to prepare chiral PANI, poly(*o*-toluidine) (POT), and poly(*o*-anisidine) (POA) with *S*-CSA as the dopant. Due to steric hindrance, the substituent in the monomer unit could not only affect the conformation of CP chains, but also change the doping degree of the products. Accordingly, the microstructure, crystallinity, and chiroptical

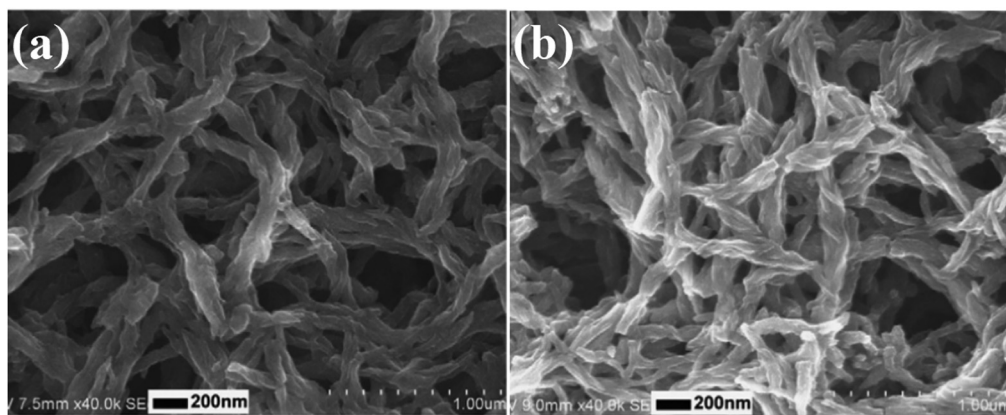


Fig. 1 (a and b) SEM images of helical PANI nanofibers prepared by the electropolymerization of aniline in the presence of *S*-CSA (a) and *R*-CSA (b) as the dopants. Reprinted with permission from ref. 29. Copyright 2010 Elsevier.

activity of the obtained products could also be adjusted by the steric hindrance caused by the substituent. Relatively speaking, the steric effects induced by the methyl substituent of the CP chain was found to be larger than those induced by the methoxy group in the *ortho* position. It was found that the steric effect increased in the order of PANI < POA < POT, while the doping level decreased.

**2.1.2.2. Induction of chiral doping acid through the chemical polymerization route.** Chiral PANI nanomaterials with different morphologies have been synthesized by the chemical polymerization of monomers in the presence of chiral doping acids, such as L-phenylalanine (L-Phe).<sup>31</sup> However, CSA has been the most frequently used chiral doping acid for inducing the chirality or chiroptical properties of CP nanomaterials.<sup>32–44</sup> It is well known that APS is often employed as the oxidizing agent in the oxidation polymerization of aniline, which can be reduced to the sulphate anion by the oxidation of aniline. In the reaction system including CSA, the sulphate anion may often compete with the CSA anion to interact with the newly produced oligomer or PANI chains driven by electrostatic attractions, which may affect the chiral conformation of polymer chains. For weakening this influence, an aniline oligomer is often introduced into the preparation system, which can interact with the chiral dopant and may assume the initial chiral conformation prior to the polymerization reaction.

Earlier, Li *et al.* developed an oligomer-assisted route to synthesize optically active PANI nanofibers in concentrated CSA solutions with APS as the oxidant.<sup>38</sup> As the final product, a dark-green viscous suspension was obtained *via* an optimized synthesis procedure, which was composed of PANI nanofibers (Fig. 2a). Evidently, these nanofibers were further entangled and twisted to form a fiber network. The experimental parameters could be employed to adjust the molar ellipticity of these PANI nanofibers varying by 5 orders of magnitude. The chirality of PANI nanofibers was found to increase with the aniline/CSA ratio. In the chemical polymerization reaction, aniline oligomers (Fig. 2c) might play the role of a seed in the generation of chiral PANI, since they could be easily oxidized with APS than the aniline monomer. With a relatively high

anisotropy factor, the trimer (b2, b6) could be rapidly oxidized and polymerized with the aniline monomer to synthesize chiral PANI.

Later, it was found that PANI twisted nanofibers were also produced *via* the chemical polymerization of monomers induced by chiral *R*- or *S*-CSA without an aniline oligomer.<sup>39,40</sup> For instance, Yan *et al.* reported the successful synthesis of chiral PANI in the presence of *R*-CSA and studied the effect of  $[R\text{-CSA}]/[\text{An}]$  ratio on the morphology of chiral PANI nanostructures.<sup>39</sup> With the  $[R\text{-CSA}]/[\text{An}]$  ratio of 1/2 or 1, the chemical polymerization of aniline could produce dendritic PANI tubes, while twisted nanofibers were formed at higher  $[R\text{-CSA}]/[\text{An}]$  ratios (such as 5 or 80). It was suggested that *R*-CSA might form micelles with aniline when its concentration was sufficiently high, which favored the formation of twisted nanofibers. It was found that the produced PANI chains were in the doped state and exhibited extended conformations. The CD data of the obtained products confirmed that PANI chains should assume helical conformation with single-handedness, which could be ascribed to the chiral induction function of *R*-CSA through H-bonding and ionic interactions.

Usually, by using *R*-CSA as the chiral doping acid in the preparation process, right-handed PANI can be obtained with stable conformation. However, Yan *et al.* found that *R*-CSA could also induce left-handed CPs by the copolymerization of aniline and *m*-toluidine (*m*-An) (Fig. 3a).<sup>41</sup> In the typical chemical polymerization route, one aniline molecule reacts with another one by the linking of the amino group of the first unit and the *para*-position of the phenyl ring of the second unit. When a methyl group is introduced into the second unit, the amino group of aniline is still linked with the *para* position of the aniline derivative [such as *m*-An or *o*-toluidine (*o*-An)] to form a dimer. However, the phenyl ring of the derivative should rotate by a given angle to free its amino group for the subsequent linking reaction. Due to steric hindrance from the methyl group in the aniline derivative, *R*-CSA as the dopant may interact with the amino end along the right-handed direction of the dimer *via* ionic and H-bonding interactions. Therefore, the succedent linking reaction of the monomer can occur on another amino end in the left-handed direction of the dimer (Fig. 3b). According to this proposal, it is possible that the

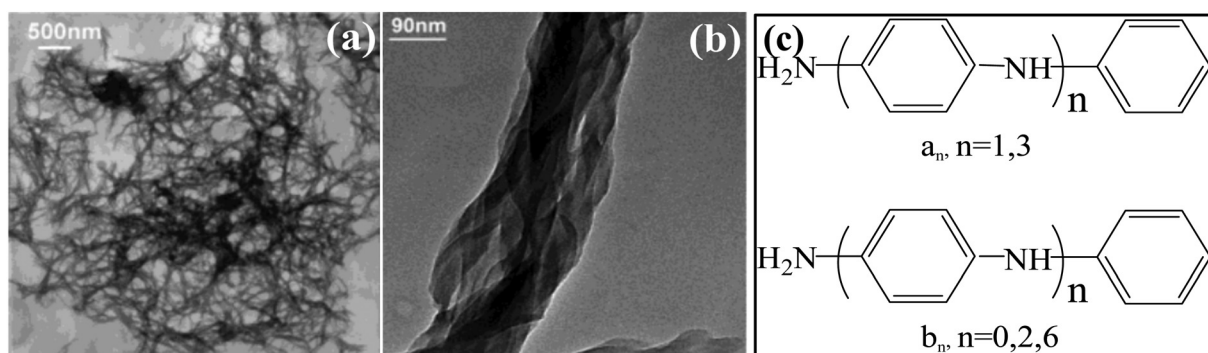


**Fig. 2** (a and b) TEM micrograph of the chiral PANI nanofiber network (a) and magnification of a fiber bundle with embedded helical nanofibers (b). (c) Molecular structures of phenylamine-capped oligomers ( $a_n$ ) and amine-amine-capped oligomers ( $b_n$ ). Reprinted with permission from ref. 38. Copyright 2004 American Chemical Society.

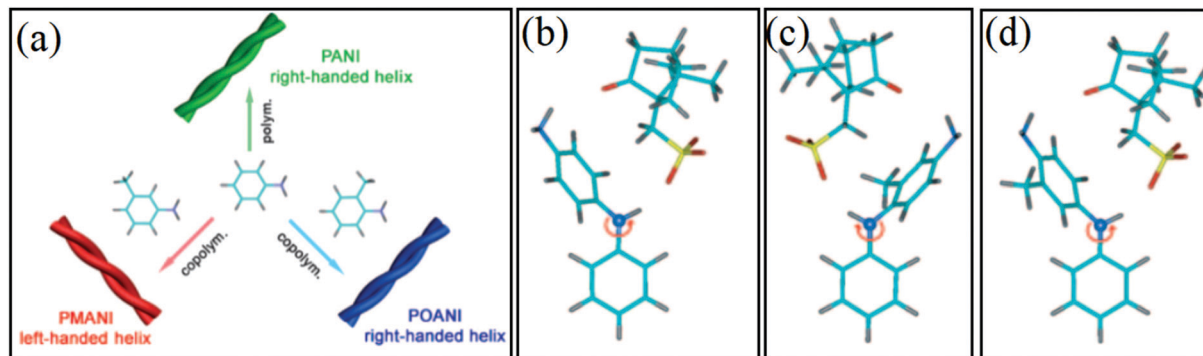


Fig. 3 (a) Schematic representation of the supramolecular chirality tuning of PANI by methyl substitution. (b–d) Theoretical models of the stable forms of dimers of (b) An–An, (c) An–*m*-An, and (d) An–*o*-An with *R*-CSA as the dopant in the polymerization process. The N atom near the reacting position is indicated by a purple ball. The N atoms in (c) and (e) exhibit left-handed chirality, while the N atom in (d) exhibits right-handed chirality. Reprinted with permission from ref. 41. Copyright 2009 John Wiley and Sons.

copolymerization of aniline and aniline derivative results in the left-handed conformation and even left-handed twisted nanofibers in the reaction system with *R*-CSA as the dopant. As found in their experiments, right-handed nanofibers could still be produced in the copolymerization system of aniline as well as *o*-An; however, the reaction of aniline and *m*-An can yield left-handed nanofibers. Helical inversion can be attributed to the hindrance of the methyl group at the *meta* position of the phenyl ring. In fact, the copolymers of aniline with *m*-An (PMANI) and that of aniline with *o*-An (POANI) yielded identical chemical components. Therefore, chiral reversal can be attributed to steric hindrance instead of the chemical components. For pure PANI and POANI nanofibers, only right-handed helical nanofibers were observed, while left-handed helical nanofibers became predominant for  $[m\text{-An}]/[\text{An}] = 1 : 10$ .

Besides single-handed helical nanofibers, the helical heterojunctions of PANI nanofibers were produced *via* the copolymerization of aniline and *N*-methyl aniline (*N*-An) with *R*-CSA as the dopant (Fig. 4).<sup>42</sup> By fine-tuning the *N*-An/An molar ratio, the handedness of the nanostructures (helical heterojunction) can be

reversed in one helical nanofiber. By altering the  $[N\text{-An}]/[\text{An}]$  ratio from 1 : 10 to 1 : 2, the CD peaks at 435 nm changed from negative to positive, confirming the conformation reversal of the copolymer chain. Moreover, the morphology of the obtained nanofibers was found to change from right-handed to left-handed (Fig. 4a and b). When the  $[N\text{-An}]/[\text{An}]$  molar ratio was modified to 1 : 2.5, it was found that the product exhibited certain interesting helical nanofibers that exhibited both left-handed and right-handed lengths. The junction between the left-handed and right-handed lengths exhibited a heterojunction character. It was suggested that the formation of such a helical heterojunction might be due to the specific reaction system. The steric hindrance of the methyl group of *N*-An might affect the copolymerization of aniline and *N*-An, further controlling the helical direction of the nanofibers. Fine-tuning the experimental parameters (such as monomers ratio and dopant concentration) play a key role in the fabrication of a helical heterojunction.

In addition, it has been reported that the steric effect caused by a substituent could induce chiral reversal from right-handed to left-handed nanohelices, which was followed by a

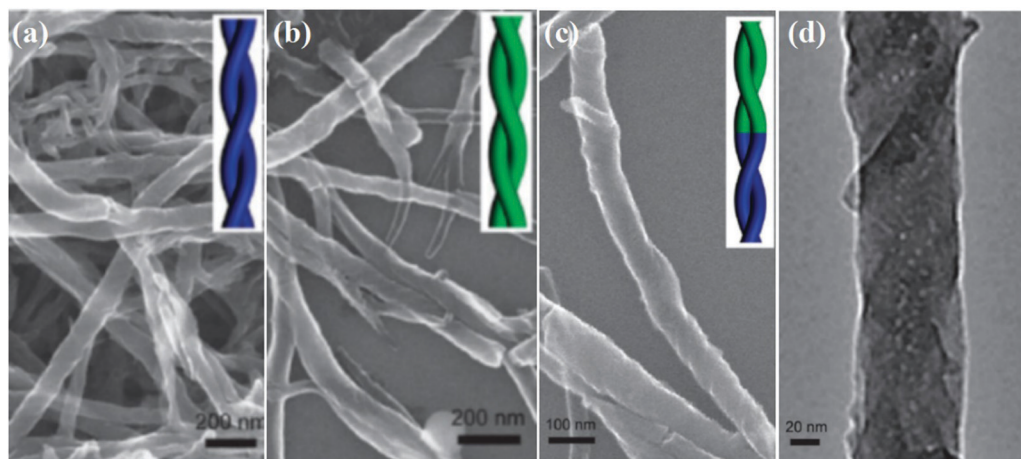


Fig. 4 (a and b) SEM images of helical PANI nanofibers obtained using (a) *R*-CSA and (b) *S*-CSA as the dopants at  $[N\text{-An}]/[\text{An}] = 1 : 2.5$ , respectively. (c) SEM and (d) TEM images of PANI helical heterojunctions obtained using *R*-CSA as the dopant at  $[N\text{-An}]/[\text{An}] = 1 : 2.5$ . Reprinted with permission from ref. 42. Copyright 2012 Royal Society of Chemistry.



conformational change from an extended long chain to a compact coil.<sup>43</sup> Chiral *ortho*-substituted PANIs, such as POA, POT, poly(*o*-ethylaniline) (POE), poly(*o*-chloroaniline) (POC), and their copolymers with aniline, have been prepared by chemical polymerization with CSA as the dopant in an aqueous solution. Evidently, *ortho*-substituted PANIs always exhibit an opposite chirality feature with respect to conventional PANI without any substitutes. With regard to these copolymers, their chirality was usually related to the steric hindrance of the substituent groups. On the other hand, increasing the content of the aniline derivative in the monomer mixture could enhance the steric effect, resulting in chiral reversal in the product. In other words, introducing a substituent at the *ortho* position of the aniline unit could be used to facilitate control the chirality of CPs.

Recently, Li *et al.* developed a new approach to control the chirality, namely, the concentration of chiral doping acid (*S*-CSA) could be employed to tune the handedness of the PANI twisted nanofibers in an oligomer-assisted polymerization reaction.<sup>44</sup> In their preparation modality, aniline oligomer comprising two amino group on its ends (2AO) was introduced into the reaction system to assist the chemical polymerization process. As reported, left-handed PANI nanofibers could be produced with lower *S*-CSA amounts (Fig. 5a), while the polymerization reaction at concentrated *S*-CSA afforded right-handed PANI nanofibers with the other experimental conditions remaining unchanged (Fig. 5b). Again, the CD data indicated that the chirality inversion of the PANI nanofibers depended on the  $[S\text{-CSA}]/[\text{aniline}]$  ratio. To illustrate such chirality inversion, two interaction models between the aniline oligomer and *S*-CSA were proposed for different dopant usages (Fig. 5c). At low  $[S\text{-CSA}]$  concentrations, one CSA molecule might form two H-bonding interactions with the two amino groups at the ends of one 2AO molecule. Obviously, the 2AO molecule would curve for interacting with one dopant molecule, exhibiting curved conformation. At high  $[S\text{-CSA}]$  concentrations, one 2AO molecule can interact with two CSA molecules at the two amino ends, where the oligomer would assume an expanded and

twisted structure. Two oligomer molecules with two different conformations would act as polymerization seeds for inducing the growth of PANI chains. A curved 2AO seed might induce the left-handed conformation in the prepared polymer chain, which further afforded left-handed nanofibers. Accordingly, right-handed PANI nanofibers could be obtained from the induction and propagation of the twisted and expanded 2AO molecules. When *S*-CSA was replaced by *R*-CSA, a similar phenomenon could be observed in the experiments. Besides, it was found that the polymerization temperature (high or low) could also be used to adjust the handedness of the obtained PANI nanofibers.

**2.1.2.3. Induction of chiral doping acid via self-assembly.** In a typical synthesis process, PANI in the emeraldine base form is initially synthesized *via* the chemical polymerization of aniline with the APS oxidant, and the obtained PANI emeraldine base powder is immersed in deionized water for a given time (*e.g.*, 24 h) and then vacuum-filtered. Then, the hydrated powder is mixed with a chiral doping acid (*e.g.*, CSA) in a good solvent (such as NMP). The solution is maintained at room temperature for a given time (*e.g.*, 48 h) before filtering. Finally, PANI/CSA thin films are cast on quartz slides using the filtrate; chiral PANI can be subsequently obtained. Using the above method, Mire *et al.* found that certain amino acids (such as glycine, *L*-tyrosine, *etc.*) could induce and stabilize the chiroptical properties of PANI films *via* the self-assembly process.<sup>45</sup>

Another self-assembly approach can be described as follows: chiral acid-doped PANI can be firstly prepared *via* the chemical polymerization of aniline in the presence of enantiomeric CSA as the chiral doping acid. Then, the prepared chiral PANI was dissolved in a good solvent to form a solution, followed by the addition of a poor solvent to the initial self-assembly process. For achieving self-assembly of the polymer chains, the volume ratio of the good solvent to poor solvent ( $[G]/[P]$ ) should be precisely controlled during the experiment. The mixed solution is normally acutely stirred or vibrated for several minutes and then allowed to stand for several hours. During the mixing process, PANI polymer chains with optimized conformations

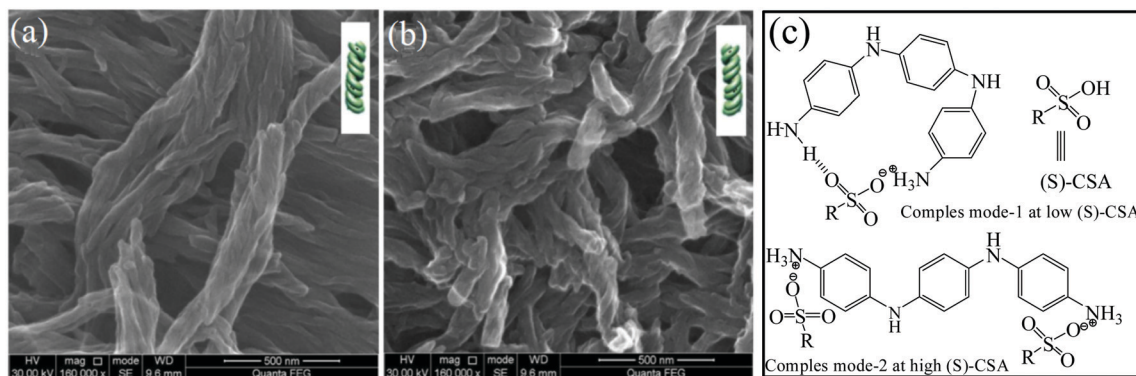


**Fig. 5** (a and b) SEM images of helical PANI nanofibers synthesized by 2AO-assisted polymerization in the presence of *S*-CSA. (a)  $[S\text{-CSA}]/[\text{AN}] = 1.90$ ; (b)  $[S\text{-CSA}]/[\text{AN}] = 3.00$ . (c) CD (up) and UV-vis (down) spectra of water-dispersed chiral PANI nanofibers prepared using *S*-CSA in the presence of 2AO oligomers. (c) Chemical structures of the aniline oligomers and the speculated interaction mode of the aniline oligomers with *S*-CSA. Reprinted with permission from ref. 44. Copyright 2018 Elsevier.





Fig. 6 (a–d) SEM images of chiral PANI nanorices, ordered hexagonal microplates, and nanowires at different [G]/[P] ratios: (a) 50/50; (b) and (c) 40/60; (d) 30/70. Reprinted with permission from ref. 46. Copyright 2010 American Chemical Society.

can aggregate and assemble, thereby minimizing the energy of the system. As a result, supramolecular assemblies were phase-separated from the liquid phase and deposited at the bottom of the reaction vessel. Using the mixed solvent of tetrahydrofuran (THF) and  $\text{CHCl}_3$  as the good solvents and methanol as the poor solvent, PANI nanorices and their 2D hexagonal microplates were formed *via* the abovementioned method, as reported by Yu *et al.*<sup>46</sup> By changing the [G]/[P] ratio from 50/50 to 40/60 and 30/70, the microstructures of the obtained products could be changed from rice-like nanostructures to hexagonal plate-like microstructures and twisted nanowires (Fig. 6a–d). Notably, hexagonal plate-like microstructures obtained at [G]/[P] = 40/60 was found to be made up of shoulder–shoulder nanorices. Interestingly, all the three products prepared at different [G]/[P] ratios exhibited positive Cotton effects in their CD spectra, while their solutions in a good solvent showed negative CD signals. Evidently, PANI chains in solution and nanostructures should have different helical conformations. In the nanostructures, strong intermolecular interactions among the polymer chains would change the conformation and might drive the ordered arrangement of PANI, thereby resulting in their helical stacking. The chiral conformation of PANI chains played a key role in their helical stacking as well as the formation of nanorices.

In their continuing investigations, they reported the fabrication of single-handed helical PANI microfibers with a length of over 20  $\mu\text{m}$  at a [G]/[P] ratio of 35:65 using a similar self-assembly method.<sup>47</sup> In this fabrication method, chiral CSA molecules not only acted as the dopant in the chemical polymerization process to increase the solubility of PANI, but also induced the chiral assembly of PANI since their steric

hindrance induced the polymer chains to assume chiral conformation for aggregation. Evidently, using *S*-CSA as the dopant afforded left-handed helical fiber-like microstructures of PANI, while doping *R*-CSA into PANI could induce the formation of right-handed microfibrils (Fig. 7). In addition to the opposite helical chirality, left- and right-handed helical microfibrils had an opposite Cotton effect, as evident from the CD spectra. Evidently, the chirality of the helical microfibrils should be related to the chiral doping acid. Further, they found that the obtained microfibrils were actually composed of several twisted nanofibers with the same screw direction, indicative of a hierarchical assembly behavior. During the self-assembly process, PANI chains with chiral conformations were initially assembled to form small nanofibers with a helical character driven by  $\pi$ - $\pi$  stacking forces, which further merged into microfibrils because these nanofibers had the same screw direction and strong tendency toward aggregating with each other.<sup>48</sup> Due to the hierarchical assembly, the induced homochirality was gradually amplified from chiral molecules to these twisted nanostructures and then to helical microstructures.

Very recently, Yang *et al.* demonstrated that the molecular chirality in CSA-doped PANI could be transferred to the helical chirality of macroscopic PANI ribbons (Fig. 8).<sup>49</sup> First, they prepared enantiomeric CSA-doped PANI by the chemical polymerization route. Then, CSA-doped PANI chains were dissolved and self-assembled to form a submicron fiber with a helical sense by using a suitable mixed solvent, which further aggregated into a macro-membrane on a polypropylene substrate. When the membrane was immersed in a THF solvent, it could be peeled from the substrate to form macro-strips. If the THF solvent was replaced by an isopropanol (iPrOH)/THF mixed

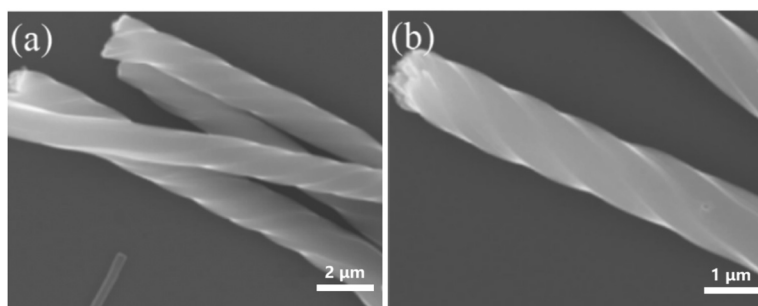


Fig. 7 SEM images of helical PANI microfibrils induced by (a) *S*-CSA as the dopant and (b) *R*-CSA as the dopant. Reprinted with permission from ref. 47. Copyright 2014 American Chemical Society.



**Fig. 8** (a) Illustration of the structure of the hierarchical components of the macroscopic assemblies of a macroribbon. The mirror-image symmetrical left- and right-handed macroribbons (left) consisted of aligned left-handed and right-handed nanoassemblies and microassemblies (middle) and single-handed PANI polymer doped by *S*-CSA and *R*-CSA (right), respectively. (b) Photograph of the macrostrip peeled down using THF. (c) Photograph of a helical macroribbon resulting from the stripe after adding *i*PrOH. Scale bars: 0.5 mm. SEM and atomic force microscope (AFM) images show the aligned fibrous nano- and microassemblies in the stripe. Evidently, the assemblies on the outside surface of the stripe were single-handed helical (b), but they were straight on the inside surface (c). Scale bars in the photographs in (b) and (c) are 0.5 mm; scale bar of the SEM image in (b) is 10  $\mu$ m; scale bar in the SEM image in (c) is 50  $\mu$ m; scale bars in the AFM images in (a) and (b) are 3  $\mu$ m. Reprinted with permission from ref. 49. Copyright 2018 Springer Nature.

solvent, the peeled strips curled to form single-handed helical ribbons. They found that the pitch of the screw of helical ribbons decreased with an increase in the *i*PrOH content of the mixed solvents. More interestingly, the helical chirality of the ribbons was closely related to the chirality of the CSA dopant used in the initial synthesis reaction of PANI. When *S*-CSA was used in the preparation, the resultant ribbons exhibited a left-handed helical feature, while right-handed ribbons were obtained as *R*-CSA was used as the doping acid in the early synthesis process (Fig. 8a). To reveal the curling mechanism, two surfaces of helical ribbons were observed using electron microscopy. The outside surface of the helical ribbons was composed of uniform single-handed fibrous assemblies, while almost straight fibers were found on the inside surface because of the restrictions posed by the substrate (Fig. 8b and c). From the molecular point of view, adding *i*PrOH into THF induced the intermolecular shrinkage on the surface of the stripe, which further caused the microscopic shrinkage strain along the long axis of the fibrous assemblies in the stripe. The self-assembly technique could be used to transfer the chirality of enantiomeric CSA to the helical sense of fiber-like assemblies. After that, the supramolecular chirality of helical assemblies would induce the shrinkage and curling up of the microscopic ribbons triggered by intermolecular interactions between PANI:CSA and *i*PrOH molecules.

**2.1.3. Induction of a chiral template.** It is well known that proteins as natural chiral macromolecules possess secondary helical structures, which may provide a chiral template for the preparation of CCPs. In fact, the protein-induced synthesis of CCPs has garnered considerable attention because of its easy operation and eco-friendly features.<sup>50,51</sup> Some proteins<sup>52,53</sup> have been employed in the fabrication of chiral PANI in the last two decades. When right-handed DNA was used as the chiral template, right-handed chiral PANI nanomaterials with

positive Cotton effects were usually prepared.<sup>54</sup> It is well known that most of the proteins or enzymes possess evident  $\alpha$ -helical content,<sup>55</sup> which would induce right-handed torsion or spiralism of PANI chains during the preparation process, thereby leading to positive CD signals.

Zou *et al.* used horseradish peroxidase (HRP) as a catalyst as well as a chiral template to synthesize chiral and water-soluble PANI in a bis-(2-ethylhexyl) sulfosuccinate micellar solution.<sup>56</sup> Guo *et al.* reported that inactivated or immobilized hemoglobin (Hb) could be employed as the chiral template to cause the formation of PANI materials with optical activity (Fig. 9).<sup>57</sup> They assumed that the chirality of the obtained PANI originated from the template functions of the protein used therein. Since the Hb protein was inactivated, there were several amino acid molecules present in the reaction solution, which would directly interact with the newly produced PANI chain and induce the chiral conformation. Evidently, the removal of Hb from the product did not change the chirality of the PANI materials. However, the immobilization of Hb by entrapment did not favor the polymerization of aniline as compared to that with natural Hb. Experimental results confirmed that the steric structure of protein could obviously affect the microstructure and molecular arrangement of the resultant PANI.

Insulin, which can form chiral helical superstructures under suitable solution conditions (such pH, salt, *etc.*), has also been used as a chiral template to fabricate alkoxy sulfonate poly(ethylenedioxythiophene) (PEDOT-S).<sup>58</sup> At pH 1.9, insulin could form twisted fibril superstructures with positive charges on the surface, while the sulfonate groups on the side chain of the deprotonated PEDOT-S exhibited negative charges. Driven by electrostatic attractions, PEDOT-S chains could be adsorbed onto the twisted fibril superstructures of insulin. With one-handed insulin as the chiral template, PEDOT-S with the same handedness could be prepared *via* the chemical polymerization



Fig. 9 Schematic illustration of the protein-induced synthesis of chiral conducting PANI nanospheres. Reprinted with permission from ref. 57. Copyright 2014 American Chemical Society.

of monomers. The coherence of chirality between the template and objective material indicated that the chirality of insulin was transferred to PEDOT-S; further, the assembly of PEDOT-S during preparation should be along the long axis of the insulin superstructures. This proposal could be further confirmed by the induced circular dichroism (ICD) spectra, where the positive signals of the protein were related to the positive Cotton effects of the PEDOT-S. Further, the microstructures of the PEDOT-S/insulin complex were always similar to those of the insulin protein. The obtained PEDOT-S/insulin complex was relatively stable in a diluted aqueous solution, and it could retain its helical sense when deposited onto a substrate.

In addition, chiral assemblies (such as organogelators) of amphiphilic molecules have also served as chiral templates to induce CCP superstructures *via* electrostatic interactions. Xie *et al.* synthesized helical PPY nanotubes and helical PPY nanofibers using supramolecular helical nanoribbons and chiral gels of amino acid amphiphiles as the chiral templates, respectively.<sup>59</sup> *N*-Myristoyl-L-glutamic acid (L-MGA) self-assembled into helical supramolecular structures in an ethanol/H<sub>2</sub>O mixed solvent. Driven by weak acid-base interactions, pyrrole monomers could be bound onto L-MGA in a supramolecular helix, resulting in positive charges on the pyrrole molecule. In this case, pyrrole monomers bound onto the supramolecular helix can get easily oxidized with APS, affording oligomers as seeds. These seeds could further polymerize the residual monomers in the solution to form a shell on the surface of the formed helix template. When the helix template was removed, helical nanotubes composed of pure PPY chains were obtained. Induced by the same courses, *N*-myristoyl-D-glutamic acid-PPY complex could also be formed with the opposite helical directions. Further, *N*-myristoyl-L-diglutamic acid (L-MDGA) as the gelator was dissolved in hot H<sub>2</sub>O to form a solution, which was then cooled to room temperature; finally, a hydrogel was formed. In such a gel, a large number of helices were formed by L-MDGA. When the active pyrrole monomers were bound onto the L-MDGA supramolecular structures, they would also be preferentially oxidized to form seeds. With similar growth processes, helical nanofibers of PPY could be prepared.

Very recently, chiral nematic liquid crystal (N\*-LC) prepared by mixing nematic liquid crystals and a chiral compound were reported to act as the chiral template for the fabrication of

helical polyacetylenes (H-PAs) by interfacial polymerization.<sup>60</sup> The chiral compound synthesized in this experiment comprised two segments whose helical chirality could be reversed by simply adjusting the temperature. The chiral compound was mixed with nematic liquid crystals to produce a chiral N\*-LC. When the temperature increased or decreased, the chiral compounds could change their helical arrangement, which further induced the liquid crystals to change their helical sense (Fig. 10a and b). H-PAs could be produced through an interfacial polymerization reaction of the monomer occurring in the N\*-LC. When the reaction was carried out at lower temperatures, right-handed microstructures of H-PAs could be obtained, while the left-handed morphology was found in the product prepared at higher temperatures (Fig. 10c and d). Notably, the helical direction of the obtained product was not the same as that of the chiral N\*-LC template.

## 2.2. Achiral preparation

In the above preparations involving CCP nanomaterials, chiral factors (chiral substituent, chiral doping acid, or chiral template) were usually crucial for the chirality generation of CP nanomaterials. Although the chiral assembly of some organic molecules was achieved in achiral systems,<sup>61</sup> the fabrication of CCP nanomaterials in an achiral reaction system remains a scientific challenge. Without any chiral factors, it is difficult to construct single-handed assemblies, because assembly with special orientations needs additional driving forces (such as steric hindrance). Interestingly, CP supramolecular assemblies with undefined chirality can be obtained in an achiral system. For example, Li *et al.* synthesized PANI helices with unknown optical properties by emulsion polymerization with dodecyl benzenesulfonic acid (DBSA) as the dopant as well as surfactant in an achiral system.<sup>62</sup> In another work, they reported that PANI helices with weak chiroptical properties could be prepared in the achiral mixed system including DBSA, aniline, and organic solvents. In this system, onion-like multilamellar vesicles were formed and acted as the soft template for helices.<sup>63</sup> The prepared product was found to contain both left- and right-handed PANI helices, thereby showing weak CD signals.

Recently, Zhou *et al.* synthesized twisted ribbon-like nanostructures of the aniline oligomer in an achiral system by performing the chemical polymerization of aniline in a mixed solution of iPrOH and water (Fig. 11a).<sup>64</sup> By simply changing



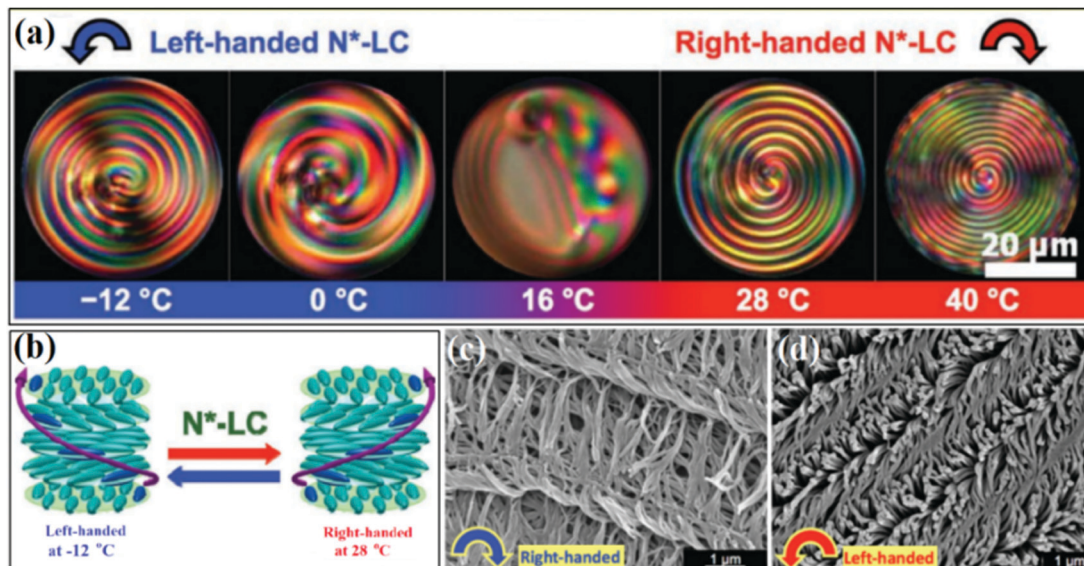


**Fig. 10** (a) Chiral inversion in the spiral optical patterns of  $N^*$ -LC during the heating and cooling processes. (b) Schematic illustration of the chiral inversion of  $N^*$ -LC. (c and d) SEM images of the H-PA films synthesized in  $N^*$ -LCs at (c)  $-12$  and (d)  $28$  °C. Reprinted with permission from ref. 60. Copyright 2020 John Wiley and Sons.

the iPrOH content in the reaction medium, the twisted orientation of the obtained nanoribbons could be adjusted. For example, most of the nanoribbons obtained with alcohol content of 35% were left-handed (Fig. 11b), whereas chemical polymerization at 45% iPrOH mainly afforded right-handed ribbon-like nanostructures (Fig. 11c). The product prepared at 35% alcohol content (left-handed nanostructures) displayed a negative CD signal at about 201 nm, while a positive Cotton

effect could be observed at 202 nm in the CD spectrum of the offspring with 45% alcohol content (right-handed nanostructures) (Fig. 11d). Chemical characterization results revealed that the major component of the products prepared with alcohol content within 35–45% was the aniline oligomer  $C_{24}H_{20}O_3N_4$ . Evidently, such an aniline oligomer had no chiral atom, indicating the presence of an achiral molecular structure. Therefore, it was deduced that the supramolecular chirality of

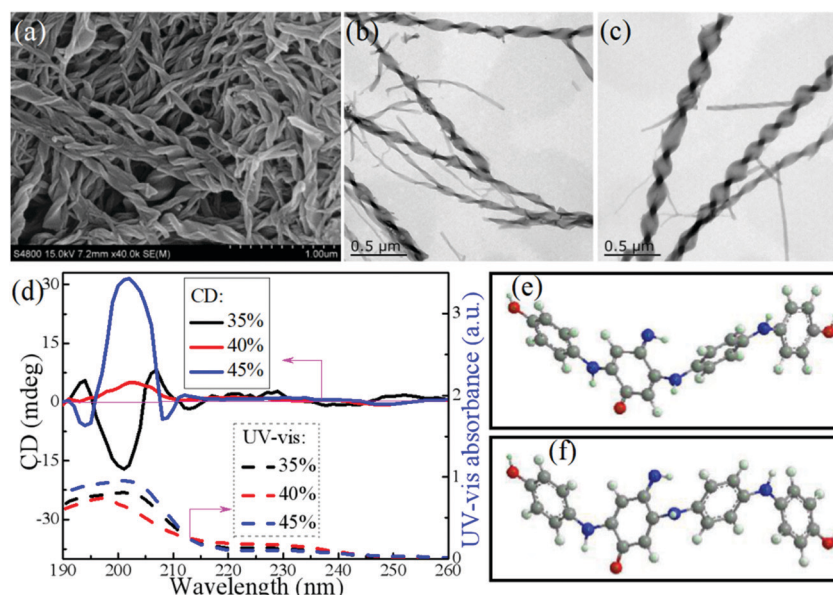


**Fig. 11** (a) FESEM image of the twisted nanoribbons at 40% iPrOH in the mixed solvent. (b and c) TEM image of the twisted nanoribbons synthesized at (b) 35% and (c) 45% iPrOH. (d) UV-vis and CD spectra of the twisted nanoribbons dispersed in an aqueous solution synthesized at different iPrOH contents. (e and f) Theoretical optimized conformation of  $C_{24}H_{20}O_3N_4$  predominated by (e) H-bonding interactions with the total binding energy of  $-251.71$   $\text{kJ mol}^{-1}$  or (f) conjugated  $\pi$ - $\pi$  stacking interactions with the total binding energy of  $-276.73$   $\text{kJ mol}^{-1}$ . Reprinted with permission from ref. 64. Copyright 2018 American Chemical Society.



the twisted nanostructures might originate from the asymmetric assembly in the system. As an asymmetric molecule along its long axis, the aniline oligomer might induce asymmetric aggregation, where the  $\pi$ - $\pi$  stacking interactions among the phenyl rings could drive self-assembly along the long axis. The conformations of the molecule should be mainly determined by the major driving force ( $\pi$ - $\pi$  stacking or H-bonding). In particular, when the major driving force was the conjugated interactions among the phenyl rings, the aniline oligomer appeared as "S"-shaped conformation (Fig. 11e). Under the H-bonding forces among the different oligomer chains, the molecular conformation of this oligomer might form a "V" shape (Fig. 11f). Because of steric hindrance, the oligoaniline molecules with different shapes can exhibit different aggregation modes. For instance, the "S"-like molecules might stack with each other into a left-handed supramolecular structure. In contrast, the right-handed model might be formed by accumulating "V"-shaped aniline oligomers. Once the generation rates for the left- and right-handed models exhibit a slight discrepancy, subsequent aggregation processes can inevitably magnify these discrepancies to generate nanofibers with the preferred helical sense. Therefore, a large number of single-handed nanotwists could be generated with obvious optical properties.

More importantly, these twisted ribbon-like nanostructures of aniline oligomers can be employed to induce the fabrication of chiral PANI nanostructures. Very recently, Zhou *et al.* found that PANI twisted nanotubes (hollow nanotwists) could be obtained when using these oligomer-based twisted nanoribbons as the reactive template (Fig. 12).<sup>65</sup> For achieving twisted nanotubes, a small quantity of hydrochloric acid was introduced into the reaction system. Using similar experimental conditions, they prepared twisted nanoribbons during the initial stages of the reaction, which further evolved into

twisted nanotubes by the subsequent chemical polymerization of the aniline oligomers. The obtained twisted nanotubes exhibited well-defined left- or right-handed hollow structures (Fig. 12a-c). Evidently, the addition of hydrochloric acid caused the evolution from solid twisted nanobelts to hollow twisted nanotubes. More importantly, it was found that the final product was PANI with higher molecular weights instead of an aniline oligomer, affording higher environmental stability and more promising applicability. As an initial template, the twisted nanoribbons formed at an early stage of the reaction functioned as a matrix for the adsorption and arrangement of newly formed polymer chains, forming a shell. When the shell of the polymer chains was sufficiently strong, the twisted ribbon-like core of the oligomer would get dissolved into the solution for continued growth. In this way, a twisted shell (tube) comprising PANI chains could be constructed, and the core of the aniline oligomers disappeared (Fig. 12d). Similar to the twisted nanoribbons, the twisted direction of the PANI nanotubes could still be tuned by adjusting the iPrOH content in the mixed solvent. By tuning the iPrOH content, left-handed PANI hollow nanotwists could be produced at 35% iPrOH, showing a negative Cotton effect; however, the right-handed PANI hollow nanotwists prepared at 45% iPrOH displayed a positive Cotton effect.

### 3. Applications in enantioselective recognition

The enantioselective recognition and separation of CCP nano-materials may be one of the most promising applications because of the high efficiency in obtaining pure enantiomers in their mixtures. Generally, the two different enantiomers of the drug candidates show completely distinct pharmacological

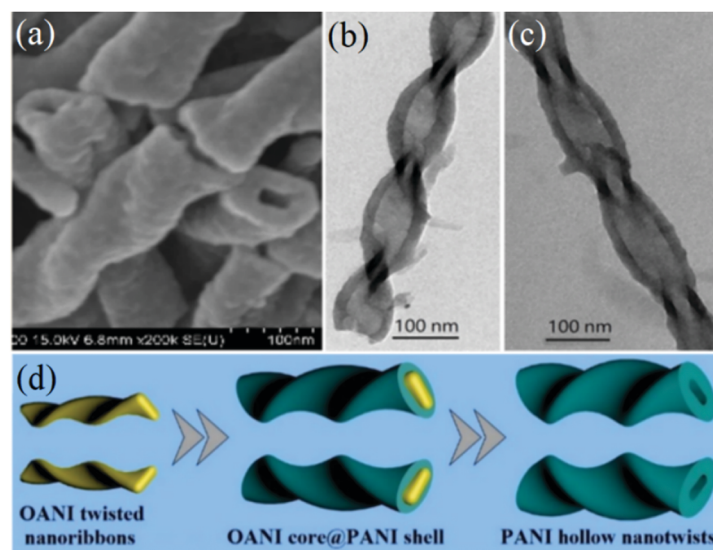


Fig. 12 (a) FESEM image of PANI twisted nanotubes synthesized in HCl/iPrOH/water mixed solvent. (b and c) TEM images of left- and right-handed twisted nanotubes. (d) Schematic diagram illustrating the evolution from OANI twisted nanoribbons to PANI twisted nanotubes. Reprinted with permission from ref. 65. Copyright 2019 American Chemical Society.

effects. For safety and therapeutic effects, a pure enantiomer should be an optimum selection instead of racemic mixtures. Therefore, the enantioselective recognition and separation toward chiral compounds become very crucial in the field of pharmaceuticals and biotechnology. The appearance of CCP nanomaterials has opened new avenues toward achieving these goals.

### 3.1. Enantioselective separation

CCPs with optical activity have shown promising potential as novel chiral stationary phases for the chromatographic separation of enantiomeric chemicals. With relatively high specific surface areas, CCP nanomaterials are anticipated to possess excellent abilities toward enantioselective separation applications. For example, PANI has the potential to act as a more general host matrix for various chiral molecules due to its doping/dedoping properties. Huang *et al.* reported that chiral PANI in the emeraldine base form could be employed to separate a racemic mixture of amino acids into their enantiomeric forms.<sup>66</sup> Besides, chiral poly(3,4-ethylenedioxythiophene) prepared in the presence of a chiral anion could be used to chirally separate *R*- and *S*-mandelic acid using CV and squarewave voltammetry.<sup>67</sup> Evidently, the protons of the protonated acid transferred between the solution and chiral PEDOT-modified electrode. These may have potential applications in the high-pressure liquid-chromatography-based enantioselective analysis of chiral chemicals.

Recently, Zhou *et al.*<sup>64</sup> reported that the twisted ribbon-like nanostructures of an aniline oligomer could be utilized for the chiral recognition and separation of phenylalanine (Phe). In the incubation experiment, chiral ribbon-like nanostructures were firstly introduced into the solution of racemic Phe at a given concentration. After mixing for a period of time, the dispersion solution was filtered to separate the filtrate liquid and filter residue. Then, this liquid was measured by CD and UV-vis techniques to estimate the enantiomeric species and concentration of residual amino acids. Based on the measurement results, it was found that left-handed ribbon-like nanostructures of the aniline oligomer could adsorb more *L*-Phe than *D*-Phe from the racemic mixture, while more *D*-Phe was removed from the mixture using right-handed nanostructures. The enantioselective uptake of twisted ribbon-like nanostructures toward racemic Phe can be ascribed to the strong binding interaction between the aniline oligomer and amino acid, as well as their matching spatial geometries. This binding interaction might include the hydrophobic force and H-bonding interactions between the two species. Since the chiral species had a given spatial structure, the spatial matching degree for aniline oligomer and Phe enantiomer could influence the intermolecular interactions and contacting area. Once the oligomer molecule was found to be suitable for the Phe enantiomer with regard to molecular conformation, the interaction and binding between them could be enhanced, resulting in enhanced uptake. In contrast, the binding driving forces would be reduced for unmatched conformations; therefore, only a few enantiomers were removed.

When compared with the twisted nanoribbons of aniline oligomers, PANI twisted nanotubes possessed larger specific surface area and better environment stability due to their higher molecular weight, thereby exhibiting more efficient ability for enantioselective separation.<sup>65</sup> The incubation experiment of PANI twisted nanotubes was performed in a way similar to that for the twisted nanoribbon of the aniline oligomer; CD and UV-vis techniques were employed to detect the filtrate liquid. With tryptophan (Try) as an example, it was found that PANI with left-handed twisted nanotubes exhibited better removal ability toward *L*-Try, while *D*-Try preferred to adsorb onto the surface of PANI right-handed twisted nanotubes. In particular, the enantiomeric excess [ee (%)] value of PANI nanotubes with more left-handed structures toward racemic Try was evaluated to be about 72.6%, while it was about 37.5% for right-handed PANI nanotubes. For recovering the amino acid, after the initial incubation experiments, the incubation mixture was filtered, and the filter residue was added into an aqueous solution of low-concentration inorganic acid. After that, the mixtures were filtered again to obtain the new filtrate liquid, which was again subjected to CD and UV-vis techniques to estimate the amount of amino acids. Evidently, most of the Try adsorbed onto the PANI twisted nanotubes ( $\geq 90\%$ ) could be desorbed by the above method. More importantly, single-handed PANI nanotubes that were subjected to the desorption experiment were able to again adsorb and selectively remove Try according to the chiral character. Fig. 13a shows the ee (%) values of single-handed PANI twisted nanotubes toward racemic amino acid Try for four cycles, revealing high stability of the chiral nanotubes toward enantioselective separation. Besides, PANI nanotubes with a single-handed character could also separate racemic Phe, glutamic acid (Glu), and alanine (Ala) (Fig. 13b). Evidently, such PANI chiral nanotubes exhibited better enantioselective separation ability toward four amino acids than the twisted nanoribbons of the aniline oligomer.

### 3.2. Enantioselective sensing

Molecularly imprinted polymers (MIPs) that act as a tool for the recognition and separation of enantiomeric chemicals have garnered considerable interest. An approach with CPs was explored by Deore *et al.*<sup>68</sup> for the first time. In their experiment, an overoxidized PPY film was imprinted with *L*-glutamate; thereafter, the PPY film could be used to distinguish between *L*- and *D*-glutamic acid. They found that the PPY film as the template could repeatedly recognize *L*-glutamate more than ten times using different methods (such as electrochemical and fluorescence techniques). Contrary enantioselectivity was exhibited for a similar PPY MIP templated with *D*-glutamic acid. The PPY films were also found to show enantioselectivity toward other chiral amino acids. An advantage of these PPYs over MIPs based on conventional polymers might be the fact that the complementary chiral cavity could be simply constructed with the simultaneous expulsion of the anionic template species *via* an electrochemical overoxidation/dedoping process. Using a similar preparation method, PPY MIPs fabricated

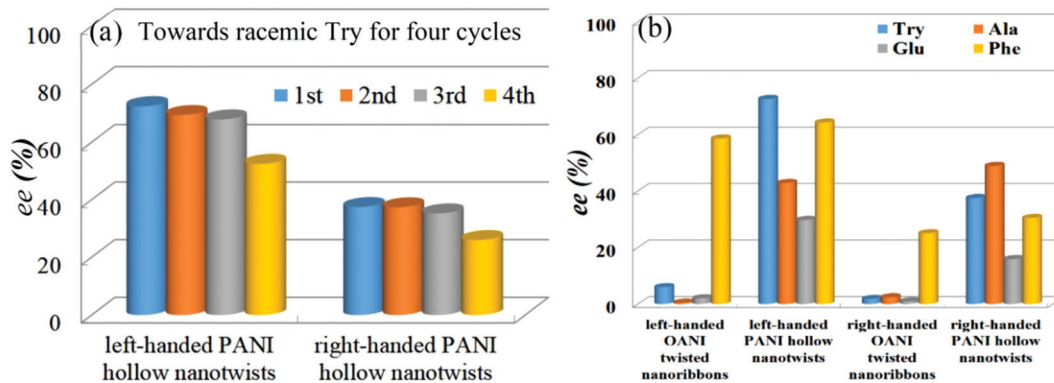


Fig. 13 (a) Histogram of ee (%) values of single-handed PANI hollow nanotwists toward racemic Try for four cycles. (b) Histogram of ee (%) values of single-handed OANI twisted nanoribbons and PANI hollow nanotwists using four racemic amino acid mixtures. Reprinted with permission from ref. 65. Copyright 2019 American Chemical Society.

with L-lactate could also be obtained and used for chiral separations.<sup>69</sup> The latter imprinted PPY was modified onto carbon fibers that was packed into an electromodulated column, which exhibited outstanding enantioselectivity for the uptake of L-amino acids over D-amino acids. Other PPY MIPs fabricated with L- and D-tyrosine<sup>70</sup> or L- and D-aspartic acid<sup>71</sup> were also reported with relatively high enantioselectivities for amino acids.

Chiral PPY nanowires doped with chiral CSA molecules have been used as the enantioselective matrix for chiral Phe.<sup>72</sup> In this matrix, multiple noncovalent interactions between CSA molecules and PPY chains mainly included electrostatic force and H-bonding interactions, which could provide multiple anchoring positions in chiral recognition. Evidently, the enantioselective recognition of chiral Phe can be detected by measuring the changes in the conductivity or CD spectra. Besides, chiral emeraldine base films derived from electrochemically generated PANI-S-HCSA and PANI-R-HCSA films have been reported to show enantioselectivity toward L- and D-Phe.<sup>73</sup>

Costello *et al.* fabricated a chiral sensor using chiral poly-(3-substituted-pyrrole)s for detecting the vapor phases of enantiomers.<sup>18</sup> In this preparation strategy, they first coated the corresponding monomer onto the poly(vinylidene)-difluoride membrane (where the polymerization reaction took place in the membrane). After that, the membrane coated by CP was mounted onto two silver contacts to form a chiral sensor. When the sensors in the vapor phase were exposed to different enantiomers [such as linonene, carvone, 2-butanol, and (*R*- and *S*-menthol)], changes in the electrical resistance were detected in order to determine the species and amount of enantiomers. It was found that the sensors afforded tremendous discrimination abilities toward different enantiomers. The experimental results confirmed that these chiral substituents on the CP chain played a key role in the enantioselective sensing application. Besides, it was also reported that a sensor based on *S*-mandelate-doped PPY could be used to enantioselectively discriminate between *R*- and *S*-mandelate.<sup>74</sup>

Recently, Zou *et al.* used highly ordered and long PANI helical microfibers to fabricate a gas sensor.<sup>47</sup> First, they deposited

chiral PANI fiber-like microstructures onto a Si substrate and then moved the SnO<sub>2</sub> nanofibers as a shadow mask to attach across a single-handed PANI fiber. An 80 nm-thick gold film was then vacuum-evaporated; subsequently, the mask was removed by a probe (Fig. 14a and b). The chiral sensor based on these PANI helical fibers could exhibit good chiral sensing ability toward chiral 2-amino-hexane as the target species. In the chiral sensing experiment, a sensor with two gold electrodes at the ends was exposed to the vapor phase of 2-amino-hexane enantiomer by changing the concentrations. In chiral amino-hexane vapor at 225 ppm, the sensor based on the left-handed fiber exhibited evident enantioselective recognition toward the amino-hexane, whose response to racemic amino-hexane was found to be between those for the two enantiomers. It was suggested that the ability of the helical microfibers could originate from the intermolecular interactions between CSA and chiral amino-hexane. Since the chiral molecules have relatively stable steric spatial conformations, the interaction among them can be strengthened if their conformations match. On the contrary, unmatched spatial structures can weaken the intermolecular interactions. With regard to the left-handed PANI fibers doped with *S*-CSA, the *S*-CSA molecule exhibited spatial conformations similar to those of *S*-amino-hexane due to the similar chiral features. Therefore, they would interact with each other; further, because of the similar molecular sizes, electron transformation from *S*-amino-hexane to PANI-*S*-CSA complex was favored (Fig. 14c). With regard to the right-handed PANI fibers doped with *R*-CSA, the inverse chiral recognition could be ascribed to the corresponding result, which was more favorable for *R*-2-amino-hexane (Fig. 14d).

Feng *et al.* used chiral PANI as the working electrode to distinguish the Ala configuration *via* the electrochemical method (*e.g.*, CV).<sup>75</sup> Once the chiral conformation of the PANI chains became the same as that of the chiral Ala molecule, they would interact with each other for transferring the electrons. As a result, the peak current of the CV as well as the corrosive current increased; accordingly, the corrosive potential and open-circuit potential decreased. Binaphthol-containing electroactive polymers were proposed by Kang *et al.* for use as

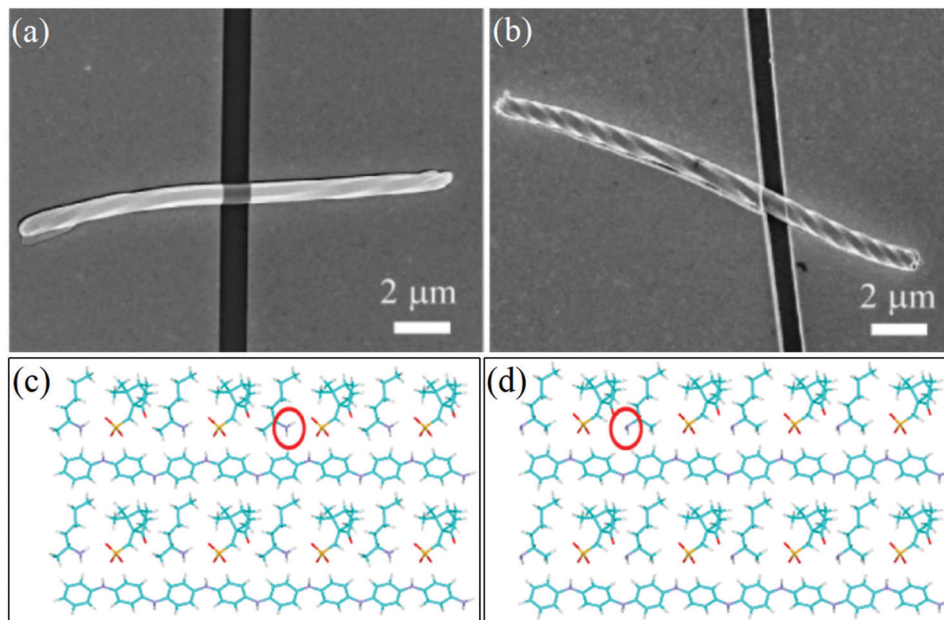


**Fig. 14** (a and b) SEM image of left-handed (a) and right-handed (b) single-helical microfiber-based enantioselective sensors. (c and d) Theoretical analysis of the enantioselective discrimination ability: (c) PANI-S-CSA inserted by *S*-2-aminohexane; (d) PANI-S-CSA inserted by *R*-2-aminohexane. Reprinted with permission from ref. 47. Copyright 2014 American Chemical Society.

chiral amine sensors to distinguish between various chiral amine analytes.<sup>76</sup>

## 4. Conclusions and outlook

In this review, we presented a comprehensive overview of CCP nanomaterials with discussions ranging from their synthesis and mechanism to applications in enantioselective separation and sensing. Two different strategies involving chiral and achiral preparations have been summarized to prepare a variety of CCP nanostructures, namely, nanoparticles, nanofilms, nanotubes, nanofibers, nanorices, hexagonal microplates, twisted nanofibers, twisted nanotubes, twisted nanoribbons, nanohelices, and so on. Although chiral nanostructures were not always found in the products, their chiroptical properties could usually be detected by the CD technique. This technique can be used to detect the differences in the molar extinction coefficients when passing left- and right-handed circularly polarized light through a sample of the compound ( $\Delta\epsilon = \epsilon_L - \epsilon_R$ ). CD measurements were also confirmed to be efficient in the detection of the conformational asymmetry of macromolecules. CD signals of the CCP nanomaterials revealed that they should contain polymer chains with asymmetrical (helical or twisted) conformations or arrangements in the materials. Control over the nanostructure and chiroptical properties of CCPs exhibited promising results with respect to their functions, which is significant for their potential applications.

Evidently, new development in the synthesis (particularly achiral preparation) and characterization of CCP nanomaterials have been seen in the past two decades. Significant progress has been achieved with regard to control over the nanostructures and optical activity of the CCPs. However, there are several

fundamental scientific problems that still remain unresolved with respect to the chirality of such materials. (1) In chiral preparation, chirality transfer from chiral factors to chiral polymer chains and twisted nanostructures are still not well understood. (2) In achiral preparation, the origin of chirality in CCP nanomaterials has been proposed, but this still needs to be confirmed by additional and key experimental results. (3) Controllable and facile fabrication of highly pure single-handed CCP nanomaterials in achiral systems remains to be a scientific challenge until now. The scientific problems encountered in these fields can be suggested to be new research directions for the future.

With regard to the application of CCP nanomaterials in enantioselective separation and sensing, past works have revealed the wonderful prospect of these materials to be applied in these fields. In fact, the enantioselective separation and sensing functions of highly efficient CCP nanomaterials have not been explored until now. In related experiments, it has been difficult to explain why CCP nanomaterials show different enantioselective abilities for chiral compounds with similar chemical structures. Therefore, additional and comprehensive studies are required to gain insights into the enantioselective mechanisms as well as to control the separation and sensing processes.

## Conflicts of interest

There are no conflicts to declare.

## Acknowledgements

The authors gratefully acknowledge financial support from the National Natural Science Foundation of China (21922202 and



21673202) and the Priority Academic Program Development of Jiangsu Higher Education Institutions.

## Notes and references

- J. Han, M. Wang, Y. Hu, C. Zhou and R. Guo, Conducting polymer-noble metal nanoparticle hybrids: Synthesis mechanism application, *Prog. Polym. Sci.*, 2017, **70**, 52–91.
- G. Ćirić-Marjanović, Recent advances in polyaniline research: Polymerization mechanisms, structural aspects, properties and applications, *Synth. Met.*, 2013, **177**, 1–47.
- C. Laslau, Z. Zujovic and J. T. Travas-Sejdic, Theories of polyaniline nanostructure self-assembly: towards an expanded, comprehensive Multi-Layer Theory (MLT), *Prog. Polym. Sci.*, 2010, **35**, 1403–1419.
- Y. Z. Long, M. M. Li, C. Gu, M. Wan, J. L. Duvail, Z. Liu and Z. Fan, Recent advances in synthesis, physical properties and applications of conducting polymer nanotubes and nanofibers, *Prog. Polym. Sci.*, 2011, **36**, 1415–1442.
- X. Lu, W. Zhang, C. Wang, T. C. Wen and Y. Wei, One-dimensional conducting polymer nanocomposites: synthesis, properties and applications, *Prog. Polym. Sci.*, 2011, **36**, 671–712.
- S. Bhadra, D. Khastgir, N. K. Singha and J. H. Lee, Progress in preparation, processing and applications of polyaniline, *Prog. Polym. Sci.*, 2009, **34**, 783–810.
- D. G. Blackmond, The origin of biological homochirality, *Philos. Trans. R. Soc., B*, 2011, **366**, 2878–2884.
- M. Liu, L. Zhang and T. Wang, Supramolecular chirality in self-assembled systems, *Chem. Rev.*, 2015, **115**, 7304–7397.
- R. Naaman, D. H. Waldeck and Y. Paltiel, Chiral molecules-ferromagnetic interfaces, an approach towards spin controlled interactions, *Appl. Phys. Lett.*, 2019, **115**, 133701.
- L. A. P. Kane-Maguire and G. G. Wallace, Chiral conducting polymers, *Chem. Soc. Rev.*, 2010, **39**, 2545–2576.
- Y. Yang, Y. Zhang and Z. Wei, Supramolecular helices: chirality transfer from conjugated molecules to structures, *Adv. Mater.*, 2013, **25**, 6039–6049.
- M. Verswyvel and G. Koeckelberghs, Chirality in conjugated polymers: when two components meet, *Polym. Chem.*, 2012, **3**, 3203–3216.
- S. Arnaboldi, S. Grecchi, M. Magni and P. Mussini, Electroactive chiral oligo- and polymer layers for electrochemical enantioselective recognition, *Curr. Opin. Electrochem.*, 2018, **7**, 188–199.
- P. C. Mondal, N. Kantor-Uriel, S. P. Mathew, F. Tassinari, C. Fontanesi and R. Naaman, Chiral conductive polymers as spin filters, *Adv. Mater.*, 2015, **27**, 1924–1927.
- H. Goto, Synthesis of polyanilines bearing optically active substituents, *Macromol. Chem. Phys.*, 2006, **207**, 1087–1093.
- D. A. Reece, L. A. P. Kane-Maguire and G. G. Wallace, Polyaniline with a twist, *Synth. Met.*, 2001, **119**, 101–102.
- S. Pleus and B. Schulte, Poly(pyrroles) containing chiral side chains: effect of substituents on the chiral recognition in the doped as well as in the undoped state of the polymer film, *J. Solid State Electrochem.*, 2001, **5**, 522–530.
- B. P. J. de Lacy Costello, M. N. Ratcliffe and P. S. Sivanand, The synthesis of novel 3-substituted pyrrole monomers possessing chiral side groups: a study of their chemical polymerisation and the assessment of their chiral discrimination properties, *Synth. Met.*, 2003, **139**, 43–55.
- G. Y. Han, G. Q. Shi, L. T. Qu, J. Y. Yuan, F. E. Chen and P. Y. Wu, Electrochemical polymerization of chiral pyrrole derivatives in electrolytes containing chiral camphor sulfonic acid, *Polym. Int.*, 2004, **53**, 1554–1560.
- G. Koeckelberghs, D. Cornelis, A. Persoons and T. Verbiest, Regioregular poly[3-(4-alkoxyphenyl) thiophene]s: evidence for a two-step aggregation process, *Macromol. Rapid Commun.*, 2006, **27**, 1132–1136.
- H. Peeters, T. Verbiest and G. Koeckelberghs, Incorporation of a conjugated side-chain in regioregular polythiophenes: chiroptical properties and selective oxidation, *J. Polym. Sci., Part A: Polym. Chem.*, 2009, **47**, 1891–1900.
- G. Koeckelberghs, M. Vangheluwe, C. Samyn, A. Persoons and T. Verbiest, Regioregular poly(3-alkoxythiophene)s: toward soluble, chiral conjugated polymers with a stable oxidized state, *Macromolecules*, 2005, **38**, 5554–5559.
- C. R. G. Grenier, S. J. George, T. J. Joncheray, E. W. Meijer and J. R. Reynolds, Chiral ethylhexyl substituents for optically active aggregates of  $\pi$ -conjugated polymers, *J. Am. Chem. Soc.*, 2009, **129**, 10694–10699.
- R. Cagnoli, M. Lanzi, A. Mucci, F. Parenti and L. Schenetti, Polymerization of cysteine functionalized thiophenes, *Polymer*, 2005, **46**, 3588–3596.
- J. C. Dobrowolskia, P. F. J. Lipińskib, S. Ostrowskia, M. H. Jamróza and J. E. Rode, The influence of the position of a chiral substituent on undecathiophene chain: A DFT study, *Synth. Met.*, 2018, **242**, 73–82.
- C. D. McTiernan, K. Omri and M. Chahma, Chiral conducting surfaces via electrochemical oxidation of L-Leucine- $\alpha$ -thiophenes, *J. Org. Chem.*, 2010, **75**, 6096–6103.
- L. Dong, Y. Zhang, X. Duan, X. Zhu, H. Sun and J. Xu, Chiral PEDOT-based enantioselective electrode modification material for chiral electrochemical sensing: mechanism and model of chiral recognition, *Anal. Chem.*, 2017, **89**, 9695–9702.
- X. Zhang and W. Song, Potential controlled electrochemical assembly of chiral polyaniline with enhanced stereochemical selectivity, *Polymer*, 2007, **48**, 5473–5479.
- S. Weng, Z. Lin, L. Chen and J. Zhou, Electrochemical synthesis and optical properties of helical polyaniline nanofibers, *Electrochim. Acta*, 2010, **55**, 2727–2733.
- E. Lee and E. Kim, Substituent effects on conformational changes in (+)-CSA doped polyaniline derivatives, *Bull. Korean Chem. Soc.*, 2013, **34**, 2111–2116.
- Y. Li, B. Wang and W. Feng, Chiral polyaniline with flaky, spherical and urchin-like morphologies synthesized in the L-phenylalanine saturated solutions, *Synth. Met.*, 2009, **159**, 1597–1602.
- R. Li, J. Dai, L. Liu, J. Wang, P. Wang, Y. Li, D. Zhou and Y. Han, Supramolecular chirality control via self-assembly of oligoaniline in the chemical oxidative polymerization process, *New J. Chem.*, 2018, **42**, 16766–16773.

- 33 Y. H. Wu, Y. Guo, N. Wang and Q. Shen, Controlling the morphology and chiroptical properties of polyaniline nanofibers by unusual interfacial synthesis, *Synth. Met.*, 2016, **220**, 263–268.
- 34 A. V. Caramyshev, V. M. Lobachov, D. V. Selivanov, E. V. Sheval, A. Kh. Vorobiev, O. N. Katasova, V. Y. Polyakov, A. A. Makarov and I. Y. Sakharov, Micellar peroxidase-catalyzed synthesis of chiral polyaniline, *Biomacromolecules*, 2007, **8**, 2549–2555.
- 35 I. S. Vasil'eva, O. V. Morozova, G. P. Shumakovich, S. V. Shleev, I. Yu. Sakharov and A. I. Yaropolov, Laccase-catalyzed synthesis of optically active polyaniline, *Synth. Met.*, 2007, **157**, 684–689.
- 36 J. Chen, B. Winther-Jensen, Y. Pornputtkul, K. West, L. Kane-Maquire and G. G. Wallace, Synthesis of chiral polyaniline films *via* chemical vapor phase polymerization, *Electrochem. Solid-State Lett.*, 2006, **9**, C9–C11.
- 37 A. Shalibor, A. R. Modarresi-Alam and R. B. Kaner, Optically active poly[2-(*sec*-butyl)aniline] nanofibers prepared via enantioselective polymerization, *ACS Omega*, 2018, **3**, 18895–18905.
- 38 W. Li and H. L. Wang, Oligomer-assisted synthesis of chiral polyaniline nanofibers, *J. Am. Chem. Soc.*, 2004, **126**, 2278–2279.
- 39 Y. Yan, Z. Yu, Y. Huang, W. Yuan and Z. Wei, Helical polyaniline nanofibers induced by chiral dopants by a polymerization process, *Adv. Mater.*, 2007, **19**, 3353–3357.
- 40 X. Li, L. Yu, L. Yu, Y. Dong, Q. Gao, Q. Yang, W. Yang, Y. Zhu and Y. Fu, Chiral polyaniline with superhelical structures for enhancement in microwave absorption, *Chem. Eng. J.*, 2018, **352**, 745–755.
- 41 Y. Yan, K. Deng, Z. Yu and Z. Wei, Tuning the supramolecular chirality of polyaniline by methyl substitution, *Angew. Chem., Int. Ed.*, 2009, **48**, 2003–2006.
- 42 Y. Yan, J. Fang, J. Liang, Y. Zhang and Z. Wei, Helical heterojunctions originating from helical inversion of conducting polymer nanofibers, *Chem. Commun.*, 2012, **48**, 2843–2845.
- 43 M. N. Anjum, L. Zhu, Z. Luo, J. Yan and H. Tang, Tailoring of chiroptical properties of substituted polyanilines by controlling steric hindrance, *Polymer*, 2011, **52**, 5795–5802.
- 44 R. Li, Y. Wang, D. Zhou, L. Liu, J. Li, Y. Li, J. Dai and Y. Han, Handedness switch of synthesized helical polyaniline nanofibers featuring the use of a single enantiomeric acid and aniline oligomers, *Polymer*, 2018, **159**, 39–46.
- 45 C. A. Mire, L. A. P. Kane-Maquire, G. G. Wallace and M. Panhuis, Influence of added hydrogen bonding agents on the chiroptical properties of chiral polyaniline, *Synth. Met.*, 2009, **159**, 715–717.
- 46 Y. Yan, R. Wang, X. Qiu and Z. Wei, Hexagonal superlattice of chiral conducting polymers self-assembled by mimicking  $\beta$ -sheet proteins with anisotropic electrical transport, *J. Am. Chem. Soc.*, 2010, **132**, 12006–12012.
- 47 W. Zou, Y. Yan, J. Fang, Y. Yang, J. Liang, K. Deng, J. Yao and Z. Wei, Biomimetic superhelical conducting microfibers with homochirality for enantioselective sensing, *J. Am. Chem. Soc.*, 2014, **136**, 578–581.
- 48 T. P. J. Knowles, A. De Simone, A. W. Fitzpatrick, A. Baldwin, S. Meehan, L. Rajah, M. Vendruscolo, M. E. Welland, C. M. Dobson and E. M. Terentjev, Twisting transition between crystalline and fibrillar phases of aggregated peptides, *Phys. Rev. Lett.*, 2012, **109**, 158101.
- 49 Y. Yang, J. Liang, F. Pan, Z. Wang, J. Zhang, K. Amin, J. Fang, W. Zou, Y. Chen, X. Shi and Z. Wei, Macroscopic helical chirality and self-motion of hierarchical self-assemblies induced by enantiomeric small molecules, *Nat. Commun.*, 2018, **9**, 3808.
- 50 B. Eker, D. Zagorevski, G. Zhu, R. J. Linhardt and J. S. Dordick, Enzymatic polymerization of phenols in room-temperature ionic liquids, *J. Mol. Catal. B: Enzym.*, 2009, **59**, 177–178.
- 51 S. Shreepathi and R. Holze, Spectroelectrochemistry and preresonance Raman spectroscopy of polyaniline-dodecylbenzenesulfonic acid colloidal dispersions, *Langmuir*, 2006, **22**, 5196–5204.
- 52 X. Hu, X. S. Shu, X. W. Li, S. G. Liu, Y. Y. Zhang and G. L. Zou, Hemoglobin-biocatalyzed synthesis of conducting polyaniline in micellar solutions, *Enzyme Microb. Technol.*, 2006, **38**, 675–682.
- 53 J. B. Chen, X. L. Kong and L. Huang, Synthesis of chiral polyaniline induced by modified hemoglobin, *Chin. J. Chem. Phys.*, 2018, **31**, 111–116.
- 54 Z. G. Wang, P. F. Zhan and B. Q. Ding, Self-assembled catalytic DNA nanostructures for synthesis of *para*-directed polyaniline, *ACS Nano*, 2013, **7**, 1591–1598.
- 55 K. Enander, D. Aili, L. Baltzer, I. Lundstro and B. Liedberg, Alpha-helix-inducing dimerization of synthetic polypeptide scaffolds on gold, *Langmuir*, 2005, **21**, 2480–2487.
- 56 F. Zou, L. Xue, X. Yu, Y. Li, Y. Zhao, L. Lu, X. Huang and Y. Qu, One step biosynthesis of chiral, conducting and water soluble polyaniline in AOT micellar solution, *Colloids Surf., A*, 2013, **429**, 38–43.
- 57 H. Guo, J. Chen and Y. Xu, Protein-induced synthesis of chiral conducting polyaniline nanospheres, *ACS Macro Lett.*, 2014, **3**, 295–297.
- 58 F. G. Bäccklund, A. Elfving, C. Musumeci, F. Ajjan, V. Babenko, W. Dzwolak, N. Solina and O. Inganäs, Conducting microhelices from self-assembly of protein fibrils, *Soft Matter*, 2017, **13**, 4412–4417.
- 59 A. Xie, F. Wu, W. Jiang, K. Zhang, M. Sunb and M. Wang, Chiral induced synthesis of helical polypyrrole (PPy) nanostructures: a lightweight and high-performance material against electromagnetic pollution, *J. Mater. Chem. C*, 2017, **5**, 2175–2181.
- 60 K. Akagi, T. Yamashita, K. Horie, M. Goh and M. Yamamoto, Chiral reaction field with thermally invertible helical sense that controls the helicities of conjugated polymers, *Adv. Mater.*, 2020, 1906665.
- 61 Z. Shen, Y. Jiang, T. Wang and M. Liu, Symmetry breaking in the supramolecular gels of an achiral gelator exclusively driven by  $\pi$ - $\pi$  stacking, *J. Am. Chem. Soc.*, 2015, **137**, 16109–16115.
- 62 C. Li, L. Yang, Y. Meng, X. Hu, Z. Wei, P. Chen and S. Zhou, Tuning PANI nanostructure by driving force for diverse capacitance performance, *RSC Adv.*, 2013, **3**, 21315–21319.

- 63 C. Li, J. Yan, X. Hu, T. Liu, C. Sun, S. Xiao, J. Yuan, P. Chen and S. Zhou, Conductive polyaniline helices self-assembled in the absence of chiral dopant, *Chem. Commun.*, 2013, **49**, 1100–1102.
- 64 C. Zhou, Y. Ren, J. Han, X. Gong, Z. Wei, J. Xie and R. Guo, Controllable supramolecular chiral twisted nanoribbons from achiral conjugated oligoaniline derivatives, *J. Am. Chem. Soc.*, 2018, **140**, 9417–9425.
- 65 C. Zhou, Y. Ren, J. Han, Q. Xu and R. Guo, Chiral polyaniline hollow nanotwists toward efficient enantioselective separation of amino acids, *ACS Nano*, 2019, **13**, 3534–3544.
- 66 J. Huang, V. M. Egan, H. Guo, J.-Y. Yoon, A. L. Briseno, I. E. Rauda, R. L. Garrell, C. M. Knobler, F. Zhou and R. B. Kaner, Enantioselective discrimination of *D*- and *L*-phenylalanine by chiral polyaniline thin films, *Adv. Mater.*, 2003, **15**, 1158.
- 67 Y. Sulaimanab and R. Katakya, Chiral acid selectivity displayed by PEDOT electropolymerised in the presence of chiral molecules, *Analyst*, 2012, **137**, 2386–2393.
- 68 B. Deore, Z. Chen and T. Nagaoka, Potential-induced enantioselective uptake of amino acid into molecularly imprinted overoxidized polypyrrole, *Anal. Chem.*, 2000, **72**, 3989–3994.
- 69 B. Deore, D. H. Yakabe, H. Shiigi and T. Nagaoka, Enantioselective uptake of amino acids using an electromodulated column packed with carbon fibres modified with overoxidised polypyrrole, *Analyst*, 2002, **127**, 935–939.
- 70 H. J. Liang, T. R. Ling, J. F. Rick and T. C. Chou, Molecularly imprinted electrochemical sensor able to enantioselectively recognize *D* and *L*-tyrosine, *Anal. Chim. Acta*, 2005, **542**, 83–89.
- 71 V. Syritski, J. Reut, A. Menaker, R. E. Gyurcsanyi and A. Öpik, Electrosynthesized molecularly imprinted polypyrrole films for enantioselective recognition of *L*-aspartic acid, *Electrochim. Acta*, 2008, **53**, 2729–2736.
- 72 J. Huang, X. Wei and J. Chen, Molecular imprinted polypyrrole nanowires for chiral amino acid recognition, *Sens. Actuators, B*, 2008, **134**, 573–578.
- 73 E. M. Sheridan and C. B. Breslin, Enantioselective detection of *D*- and *L*-phenylalanine using optically active polyaniline, *Electroanalysis*, 2005, **17**, 532–537.
- 74 M. Kaniewska, T. Sikora, R. Katakya and M. Trojanowicz, Enantioselectivity of potentiometric sensors with application of different mechanisms of chiral discrimination, *J. Biochem. Biophys. Methods*, 2008, **70**, 1261–1267.
- 75 Z. Feng, M. Li, Y. Yan, T. Jihai, L. Xiao and Q. Wei, Several novel and effective methods for chiral polyaniline to recognize the configuration of alanine, *Tetrahedron: Asymmetry*, 2012, **23**, 411–414.
- 76 S. Kang, I. Cha, J. G. Han and C. Song, Electroactive polymer sensors for chiral amines based on optically active 1,1-binaphthyls, *Mater. Express*, 2013, **3**, 119–126.